

Caveats of mean first-passage time methods applied to the crystallization transition: effects of non-Markovianity

Swetlana Jungblut¹ and Christoph Dellago¹

¹*Faculty of Physics, University of Vienna, Boltzmannngasse 5, 1090 Wien, Austria*

Using the crystallization transition in a Lennard-Jones fluid as example, we show that mean first-passage time based methods may underestimate the reaction rates. We trace the reason of this deficiency back to the non-Markovian character of the dynamics caused by the projection to a poorly chosen reaction coordinate. The non-Markovianity of the dynamics becomes apparent in the behavior of the recurrence times.

PACS numbers: 64.70.D-, 64.60.qe, 64.75.Gh

I. INTRODUCTION

In the study of activated events such as chemical reactions or first order phase transitions, the calculation of rate constants is an important task and, in the past decades, several advanced computational methods have been developed for this purpose¹⁻⁴. These methods concentrate on the rare barrier crossing events such that they are not hampered by long waiting times between events. However, these techniques are computationally demanding and it may be convenient to switch to the mean first-passage time (MFPT) or mean lifetime (MLT) methods, if it is possible to observe the reactions on the timescale of straightforward simulations. These approaches, based on a statistical description of activated events, have been around for years (see, *e.g.*, Ref. 5 for a historical view), but recently, as simulations became fast enough to produce reaction trajectories directly, they have gained popularity⁶⁻²⁶. Particularly notable is the method by Wedekind, Strey and Reguera¹⁶, which details how reaction rate constants and sizes of critical clusters can be extracted from mean first-passage times. MFPT and MLT methods have been applied to various processes including the crystallization of a Lennard-Jones (LJ) liquid¹⁹⁻²³. Here, we report a disagreement that we found between the crystallization rates computed with the MFPT (MLT) method and transition interface path sampling² (TIS). This deviation can be traced back to the non-Markovian character of the crystallization transition in terms of the chosen reaction coordinate, implying that the application of the MFPT and MLT techniques are not as straightforward as suggested in recent studies.

The main issue discussed previously concerning the applicability of MFPT and MLT techniques is the lack of timescale separation between the nucleation and growth times for processes with relatively low activation barriers^{16,25,26}. In this paper, we point out another source of error, which is related to a poor choice of the reaction coordinate. As is known from previous studies²⁷⁻³⁰, the crystallization of an undercooled LJ fluid proceeds via the formation of a crystallite with body-centered cubic (bcc) structure, which subsequently relaxes into the face-centered cubic (fcc) structure. In computational studies of this process one usually defines the number of parti-

cles in the largest crystalline cluster^{27,31} as the reaction coordinate. Although this coordinate does not contain enough information to precisely describe the progress of the reaction, it performs relatively well in comparison to other order parameters²⁹ and, in practice, it is the most convenient and widely used one. It has been shown before that a poor choice of the reaction coordinate may result in an overestimation of the reaction rate¹³. Here, however, we find that an insufficient reaction coordinate used in conjunction with MFPT method leads to an underestimation of the rate constant.

The article is structured as follows. We start with the standard analysis of the MFPT and MLT formalism and compare the obtained reaction rates with the values from TIS simulations. Then, we take a closer look at the MFPT data for the crystallization of a liquid and show that the process we consider is non-Markovian, in contradiction to the main assumption of the analysis. We explain this with the features of the crystallization transition, particularly with the lack of a good definition of the reaction coordinate. To demonstrate the issue, we consider not only the first passage but also subsequent passages and show that the behavior of these later passages indicates the onset of relaxation. Finally, we argue that the assumption of the relaxation times being negligible on the timescale of the reaction does not apply in the case of the crystallization transition.

II. SIMULATION DETAILS

We simulated a system of $N = 6668$ particles interacting via a standard truncated and shifted Lennard-Jones potential. The cutoff distance was set to $r_c = 2.5$ (in LJ units, which are used throughout the paper). The particles were confined to a cubic box with periodic boundary conditions in all directions, which was allowed to fluctuate to fix the pressure at a value close to zero ($p = 0.003257$). The evolution of the system was simulated with molecular dynamics (MD) simulation in the NpH ensemble³² with a time step of $\Delta t = 0.01$ and an enthalpy of $H = -5.11$ per particle such that the initial undercooling was about 28% ($T = 0.5$). We used Steinhardt bond order parameters³¹ with the standard scheme

proposed by ten Wolde, Ruiz-Montero, and Frenkel²⁷ to identify crystalline clusters, and monitored the progress of the reaction by considering the size of the largest crystalline cluster, n_s . Details of this analysis and of the TIS simulations^{2,33,34} are extensively described in our previous work³⁵. Mean first-passage times were calculated from a collection of 200 MD trajectories started in the initial undercooled state. For every cluster size considered, we calculated the average time the system needs to form clusters of this size or larger for the first time. Also, for every trajectory, we computed the lifetime of the undercooled state, which was defined as the time to reach a particular cluster size, well above the critical size. For this purpose, we chose the size of $n_s = 400$ and compared the resulting rate with the one obtained for $n_s = 1000$.

III. RESULTS AND DISCUSSION

In this section, we present the reaction rates computed with different methods and demonstrate that the crystallization of an undercooled LJ fluid does not comply with the requirement for a Markovian process, which the starting point of the MFPT analysis. We attribute this behavior to the fact that the nature of the crystallization transition is not completely captured by the size of the largest crystalline cluster used as reaction coordinate.

The main assumption of the MFPT and MLT methods is that the dynamics of the reaction in terms of the reaction coordinate, n_s , is described by the one-dimensional Fokker-Planck equation¹⁴ for the probability density function $p(n_s, t)$ of n_s at time t :

$$\begin{aligned} \frac{\partial p(n_s, t)}{\partial t} &= \frac{\partial}{\partial n_s} \left\{ D_0 e^{-\beta U(n_s)} \frac{\partial}{\partial n_s} \left[p(n_s, t) e^{\beta U(n_s)} \right] \right\} \\ &= -\frac{\partial j}{\partial n_s}, \end{aligned} \quad (1)$$

where j is the probability flux, D_0 is the diffusion coefficient (assumed to be constant here), U is the free energy, T is the temperature, k_B is the Boltzmann constant, and $\beta = 1/k_B T$. For an activated process with a relatively high nucleation barrier, one assumes that the system rapidly reaches a steady-state with a constant probability current

$$j = -D_0 e^{-\beta U(n_s)} \frac{\partial}{\partial n_s} \left[p_{\text{st}}(n_s) e^{\beta U(n_s)} \right]. \quad (2)$$

Here, $p_{\text{st}}(n_s)$ is the stationary distribution of states, and the reaction rate j is related to the nucleation rate J by $j = JV$.

A. Reaction rates

1. Mean first-passage time

From Eq. 2, the MFPT^{9,36} for a state with a given number of particles in the largest crystalline cluster, n_s ,

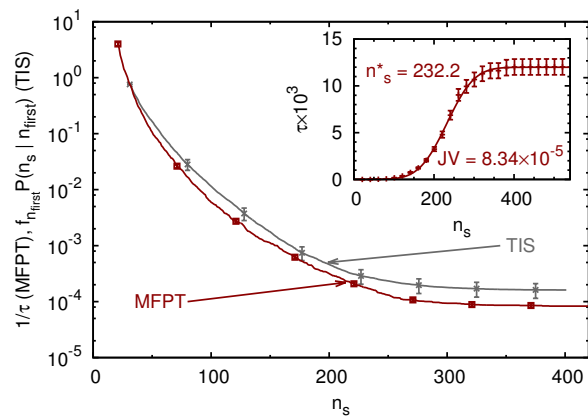


FIG. 1. The inverse of the MFPT, $1/\tau$, and the product of the flux out of the initial state and the TIS conditional probability to reach a given state, $f_{\text{first}} P(n_s | n_{\text{first}})$, as a function of the cluster size, n_s . For large cluster sizes, both curves saturate to the values of the reaction rate, JV . For clarity, errors are indicated only for selected data points. Inset: Selected values of MFPTs with errors and the fit of all data points to Eq. 4 (solid line). Also included are the values of fitted parameters JV and n_s^* .

can be calculated as

$$\tau(n_s) = \frac{1}{D_0} \int_{n_0}^{n_s} dy \exp[\beta U(y)] \int_a^y dz \exp[-\beta U(z)], \quad (3)$$

where a is the reflective boundary of the initial state and n_0 , from which the times to reach a particular cluster size are calculated, belongs to the metastable state. For the case of the crystallization transition, we set $a = 0$ (no crystallites) and $n_0 = 20$. In fact, for n_0 any value smaller than the position of the top of the free energy barrier is valid and we select this one following our definition of the initial state which we used in TIS simulations.

In the scheme proposed by Wedekind, Strey and Reguera¹⁶, the behavior of the MFPT close to the transition region is described by the function

$$\tau(n_s) = \frac{\tau_J}{2} \{1 + \text{erf}([n_s - n_s^*]c)\}, \quad (4)$$

where $\text{erf}(x) = (2/\sqrt{\pi}) \int_0^x \exp(-y^2) dy$ is the error function, n_s^* is the size of the critical cluster, and $c = \sqrt{0.5\beta |U''(n_s^*)|}$ is the local curvature at the top of the barrier. The reaction rate is then given by

$$JV = \frac{1}{\tau_J}, \quad (5)$$

where V is the volume of the system.

As can be seen in the inset of Fig. 1, Eq. 4 perfectly reproduces the MFPTs obtained in the simulations if τ_J , n_s^* , and c are used as fitting parameters. The fit yields a critical cluster size of $n_s^* = 232$, a crystal nucleation rate of $JV = 8.3 \times 10^{-5}$, and a local curvature at the top of

the barrier of $c = 0.013$. The timescales of the nucleation and growth regimes are clearly separated, as can be seen from the shape of the MFPT curve, which is displayed in the inset of Fig. 1. Also, in section III A 3, we present the lengths of the crystallizing paths, which go directly from the metastable to the crystalline states. These times the system needs to grow crystalline clusters are distinctly shorter than the MFPTs.

In Fig. 1, we plotted the inverse of the MFPTs as a function of the cluster size in comparison with the results of the TIS simulations discussed below. One can clearly see that the MFPT method underestimates the reaction rate obtained with TIS by almost a factor of two (1.92).

2. Mean lifetime

The mean lifetime (MLT)²¹ or direct observation method¹⁸ is based on the same formalism as the MFPT method, and it is expected to give the same results if the final states are well beyond the critical region³⁷. It also does not rely on the exact definition of the transition state⁸ and allows a distinction between nucleation and growth regimes²⁶. In Fig. 2, we present the probability to observe a crystallized system in a given time interval, which is fitted to the predicted Poisson distribution²¹

$$H(t|n_s \geq 400) = ht \exp(-\lambda t), \quad (6)$$

using h and λ as fitting parameters. The reaction rate JV is then equal to λ :

$$JV = \lambda. \quad (7)$$

As expected, the rate we obtain with the MLT method ($JV = 9.7 \times 10^{-5}$) is comparable to the MFPT rate. The inset of Fig. 2 also demonstrates that if we choose another value to define a crystallized system ($n_s = 1000$) the reaction rate does not change, provided we stay well above the critical cluster size. Thus, similarly to the MFPTs, the contribution of the growth times is negligible. Still, the value of the reaction rate does not coincide with the one obtained with the TIS method.

3. Transition interface sampling

The advantage of the transition interface sampling technique is that it does not depend on the definition of the reaction coordinate. One only has to be able to distinguish between the initial and the final states of the reaction and sample paths in the transition region between these states. In the TIS formalism, the crystallization rate is expressed as

$$JV = f_{\text{first}} P(n_{\text{last}}|n_{\text{first}}), \quad (8)$$

where f_{first} is the flux through the first interface considered for sampling, $n_{\text{first}} = 30$, and $P(n_{\text{last}}|n_{\text{first}})$ is

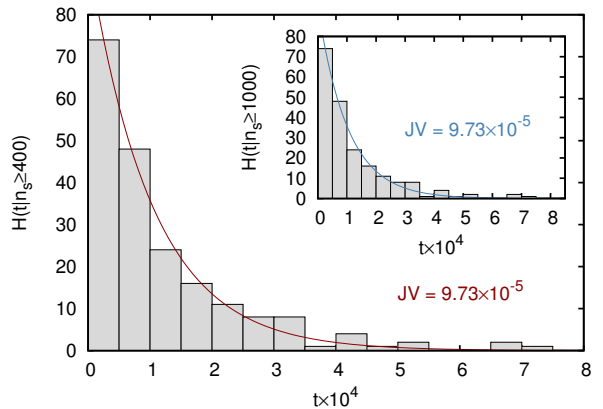


FIG. 2. Histogram of the lifetimes of the metastable state defined as $t|n_s \geq 400$ (main frame) and $t|n_s \geq 1000$ (inset) and fits to Eq. 6. Also included are the values of the fitted parameter JV .

the probability to reach the final state under the condition that the trajectory, which started in the initial phase ($n_0 \leq 20$), crossed the first interface ($n_{\text{first}} = 30$). The definition of the final state is relatively uncritical, since the probability to relax into the final state becomes constant after the system overcomes the free energy barrier. The value of the reaction rate we obtained in the TIS simulations³⁵ is $JV = (1.6 \pm 0.4) \times 10^{-4}$, which differs significantly from the rates obtained with the MFPT and MLT methods.

Still, the paths which are sampled in the TIS are essentially the same trajectories as those considered for the MFPT calculations. For example, in Fig. 3, we compare the lengths of the TIS and MFPT paths directly connecting the initial state with the respective states with a given cluster size. The length of the MFPT trajectories is restricted to the fragments of the trajectories, in which the system leaves the initial state $n_0 \leq 20$ for the last time and reaches the given state. Evidently, there is no difference in lengths between the growing paths. Also the flux from the initial state used in TIS corresponds to the inverse MFPT at the position of the first TIS interface, as can be seen in Fig. 1, where these values coincide since the probability $P(n_{\text{first}}|n_{\text{first}})$ equals unity.

In addition, we performed a commitment analysis to find the transition states of the system³⁸. The configurations with equal probabilities to reach either the initial undercooled liquid or the final fully crystalline states contain crystalline clusters with sizes between 118 and 263 particles. The critical cluster size obtained with the MFPT method lies well within this range.

4. Multiple crossings

Next, we looked at the times of subsequent passages at a given cluster size. All clusters considered here have a

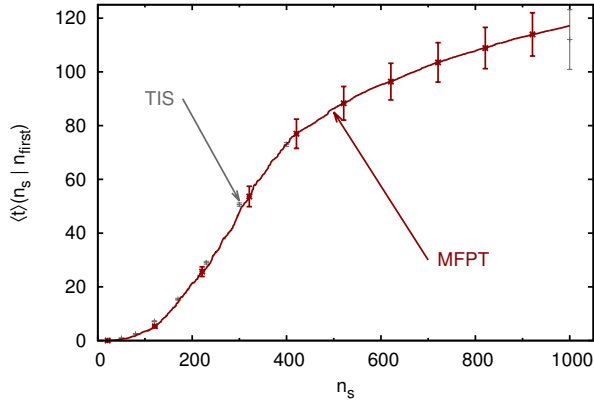


FIG. 3. Mean times to reach a particular cluster size for the first time when coming directly from the border of the initial state ($n_s = 20$). Lengths of TIS paths are evaluated at the positions of the interfaces used to calculate the crystal nucleation rate ($n_s = 50, 80, 120, 170, 230, 300, 400$), the last point ($n_s = 1000$) resulted from average over 100 crystallizing paths. MFPTs are evaluated at all cluster sizes, while errors are presented only for selected values.

finite probability to shrink to smaller sizes, which depends on the size of the cluster. Hence, particularly smaller clusters tend to fluctuate around a size region for a while, passing through an imaginary interface multiple times. We thus collected the times a certain cluster size is reached from below for the first (MFPT), second, and further times. In the top panel of Fig. 4, we plotted the corresponding averages over all trajectories for selected passages. The data for larger cluster sizes becomes increasingly noisy with the order of passage, since the number of trajectories, in which multiple crossings are observed, decreases. The shape of the obtained curves for subsequent crossings is similar to that of the MFPT, but the position of the inflection point varies with the number of passages. This behavior is expected since the integration of the process in MD is discrete in time, and the recurrence times for a state depend on the time interval Δt between configurations^{41,45,46}. In a Markovian process, described in the framework of the Fokker-Planck formalism, the position of the inflection point for the N_c^{th} passage can be approximated as (see Appendix)

$$\tilde{n}_s(N_c) = n_s^* + \frac{\sqrt{\pi}Z^{-1}}{2c^2\Delta t f(N_c)} \left\{ 1 \pm \sqrt{1 + \frac{8[c\Delta t f(N_c)]^2}{\pi Z^{-2}}} \right\}, \quad (9)$$

with $f(N_c) = N_c - 1$, c and n_s^* extracted from the fit of Eq. 4 to the MFPTs. Z is the normalization constant of the probability distribution which we use as a fitting parameter. In Fig. 4 (bottom panel), we demonstrate that the values for the position of the inflection points are relatively close to this function. However, the shape of the curve can be reproduced almost exactly by using

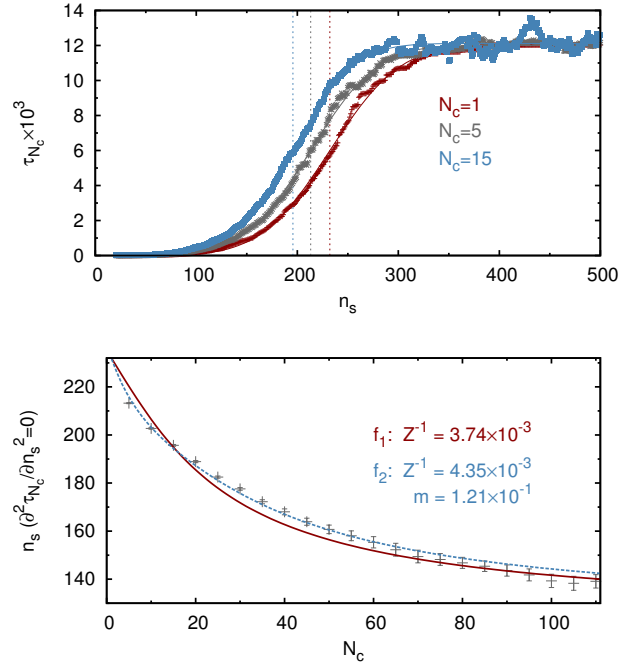


FIG. 4. Top: Mean times for 1st, 5th and 15th passages at given cluster size, n_s . Solid lines indicate fits to Eq. 4, from which we extract the positions of the inflection points. Bottom: Position of the inflection point as a function of the number of crossings, N_c , (values are extracted from corresponding fits and error bars indicate the error of the fits only). Lines are fits to Eq. 9 with $f_1(N_c) = N_c - 1$ (solid line, fitting constant Z) and $f_2(N_c) = (N_c - 1)\{1 + \exp(-m[N_c - 1])\}$ (broken line, fitting constants Z and m).

$f(N_c) = (N_c - 1)\{1 + \exp(-m[N_c - 1])\}$ with another fitting constant m . We motivate this choice with the decreasing variations of the recurrence times, which is a feature of a non-Markovian process. According to the fit shown in Fig. 4, $m \approx 0.1$ indicates that the memory effects have effectively decayed after about 10 recurrences, corresponding to a decay time of $\sim 10^3$ at the top of the barrier, which is comparable to the MFPTs. This is in accordance with the observed effect on the crystallization rate, since a shorter relaxation time would not influence the MFPT, while a longer relaxation would produce a larger discrepancy between the reaction rates computed with the MFPT and TIS methods.

5. Mean recurrence times

In the period between two subsequent passages at a given size, the number of particles in the crystalline cluster is first above and then below this value. Generally, the time to shrink to a given cluster size differs from the time to grow to this size. Thus, we define a mean recurrence time as half of the time between subsequent

crossings of an imaginary interface, at which the cluster is growing. To improve the statistics, we also average the obtained values over five subsequent passages. In Fig. 5, we thus present the data averaged over ten recurrences. Although still quite noisy, the mean recurrence times for the first passages are distinctly larger than the times for the following passages, if crystalline clusters are large enough. The difference becomes smaller as the order of passages considered increases. For a stationary distribution of states, the mean recurrence times are inversely proportional to the steady-state probabilities, $p_{\text{st}}(n_s)^{41,46}$, from Eq. 2:

$$\langle t_r \rangle(n_s) = \frac{\Delta t}{p_{\text{st}}(n_s)}. \quad (10)$$

Here, Δt is the time interval between configurations, *i.e.*, the MD integration step. As Fig. 5 demonstrates, in our case, the mean recurrence times vary with the order of visits to a given state. This finding contradicts the Markovianity assumed in the MFPT and MLT analysis, which implies that the time needed to return to a certain point should only depend on the point but not on the number of times the point has been reached before. However, after a few passages, the recurrence times become almost constant, indicating that the memory effects decline rapidly, as we have assumed in the analysis of the inflection points.

The memory effect observed in the recurrence times is most likely due to a structural relaxation not described by the reaction coordinate. The importance of the structure of the crystalline clusters has been pointed out in several works²⁷⁻³⁰, which indicate that the crystallization transition in undercooled LJ fluids follows the Ostwald's step rule³⁹. According to this rule, a metastable system does not have to relax directly into the most stable state. If there is another metastable state, the probability that the system will visit this state depends on the height of the free energy barrier between the states⁴⁰. For an undercooled LJ system, the most stable state is the face-centered cubic (fcc) structure, but the free energy barrier between the liquid and the metastable body-centered cubic (bcc) crystal is sufficiently low, such that the fluid may first freeze into the bcc structure and then relax into the more stable fcc structure.

The main message of this scenario is that there is a second important variable in addition to the cluster size, which is needed to completely describe the transition. However, we cannot deduce a precise definition for this coordinate, only that it is somehow connected to the structure of the cluster. We assume that the equilibration of the system along this coordinate requires a noticeable amount of time, in which the cluster does not grow further but is also not driven back to the initial state. As a consequence, although the trajectory is evolving, the overall reaction rate is not influenced. One could try to eliminate the non-Markovianity by using an appropriate two-dimensional reaction coordinate^{13,42,43}, but it is unclear how to do this in practice. Another approach would

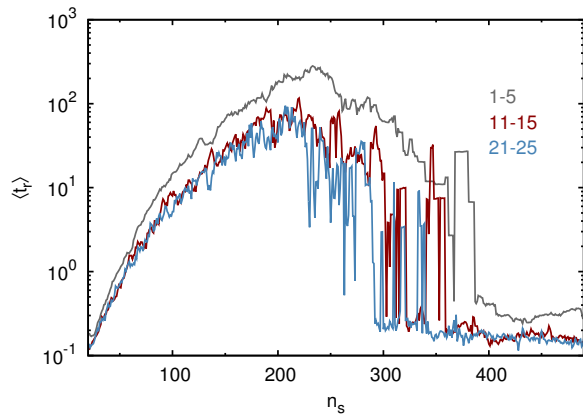


FIG. 5. Mean recurrence times for given cluster sizes calculated as half of the mean times between subsequent passages and averaged over 1st to 5th, 11th to 15th, and 21st to 25th passages.

be to keep a one-dimensional reaction coordinate and apply more sophisticated models for barrier crossing events that include memory effects, as has been done recently for the case of polymer dynamics⁴⁴.

We were particularly surprised to find discrepancies in the results obtained with different methods, because the applicability of the MFPT and MLT methods to crystallization transition has been demonstrated in several previous works¹⁹⁻²³. We presume that the differences we see are due to the relative importance of the structural transition for our system. We guess that the non-zero pressure used by other authors suppresses the impact of the structural relaxation. In other words, at zero pressure, the timescale for this relaxation becomes noticeable in comparison to the timescale of crystal nucleation.

IV. SUMMARY

We have studied the kinetics of the crystallization transition with different methods and have demonstrated that the quality of the reaction coordinate is important for the application of the mean first-passage time techniques. While previous studies placed emphasis on the importance of the timescale separation between the nucleation and growth processes, we have shown that the nature of the transition process also plays an important role. It has been shown before that the results of the MFPT calculations heavily rely on the definition of a good reaction coordinate¹³, and here we demonstrate that, at least for two-step nucleation processes like crystallization, apparently sound results of the MFPT analysis may be wrong. The examination of the subsequent passages shed light on the origin of the failure of the MFPT method, indicating that a structural relaxation of the crystalline nucleus not captured by the reaction coordinate plays an important role.

In general, the analysis of the mean recurrence times is a straightforward method to detect a non-Markovian character of the process in a given reaction coordinate. Thus, this approach provides a method to evaluate the reliability of MFPT-based techniques. It is valid for any kind of transition and, should the recurrence times demonstrate appearance of the memory effects, indicates the need for a more detailed analysis. Then, one can either try to re-define the reaction coordinate and the Fokker-Planck equation, or just use advanced simulation techniques, like TIS, which do not rely on a valid reaction coordinate.

ACKNOWLEDGMENTS

The computational results presented have been achieved, in part, using the Vienna Scientific Cluster (VSC). We acknowledge financial support of the Austrian Science Fund (FWF) within the Project V 305-N27 as well as SFB ViCoM (Grant F41).

Appendix: Position of the inflection point for the N_c^{th} passage time

We calculate the position of the inflection point for the N_c^{th} passage time in the steepest descent approximation used in the MFPT method^{16,17}. The time to reach a given cluster size for the N_c^{th} time consists of the time to reach it for the first time and $N_c - 1$ returns to this state:

$$\tau_{N_c}(n_s) = \tau(n_s) + f(N_c)\langle t_r \rangle(n_s), \quad (\text{A.1})$$

where τ is the MFPT (Eq. 4), $\langle t_r \rangle$ is the average recurrence time. Evidently, $f(N_c) = (N_c - 1)$ for constant recurrence times, which is a signature of a Markovian process. In our case, however, the system is better described by $f(N_c) = (N_c - 1)\{1 + \exp(-m[N_c - 1])\}$, where m is a fitting constant we introduce to include memory effects. In the continuous time limit⁴⁵, the recurrence time is infinitely small, even in the vicinity of the barrier. However, we consider a discrete time process^{41,46} for which this time is inversely proportional to the steady-state probabilities, $p_{\text{st}}(n_s)$, from Eq. 2:

$$\langle t_r \rangle(n_s) = \frac{\Delta t}{p_{\text{st}}(n_s)}. \quad (\text{A.2})$$

Here, Δt is the time interval, corresponding to the integration time step between configurations. Then, the second derivative of the N_c^{th} passage time is given by

$$\frac{\partial^2 \tau_{N_c}(n_s)}{\partial n_s^2} = \frac{1}{D_0} + \frac{\beta \partial U(n_s)}{\partial n_s} \frac{\partial \tau(n_s)}{\partial n_s} + f(N_c) \frac{\partial^2 \langle t_r \rangle(n_s)}{\partial n_s^2}. \quad (\text{A.3})$$

Using Eqs. 2 and A.2, we can expand the last term as

$$\frac{\partial^2 \langle t_r \rangle(n_s)}{\partial n_s^2} = f(N_c) \langle t_r \rangle(n_s) \left\{ \frac{\beta \partial^2 U(n_s)}{\partial n_s^2} + \left[\frac{\beta \partial U(n_s)}{\partial n_s} + \frac{j}{D_0 p_{\text{st}}(n_s)} \right] \times \left[\frac{\beta \partial U(n_s)}{\partial n_s} + \frac{2j}{D_0 p_{\text{st}}(n_s)} \right] \right\}. \quad (\text{A.4})$$

In the steepest descent approximation, the free energy around the top of the barrier can be written as

$$U(n_s) \approx U(n_s^*) - \frac{c^2}{\beta} (n_s - n_s^*)^2, \quad (\text{A.5})$$

and the first derivative of the MPFT is

$$\frac{\partial \tau(n_s)}{\partial n_s} = \frac{c}{j\sqrt{\pi}} e^{-c^2(n_s - n_s^*)^2}. \quad (\text{A.6})$$

Then, we insert these expressions into Eq. A.3 and set it to zero to obtain the position of the inflection point as a function of N_c :

$$0 = \frac{\partial^2 \tau_{N_c}(n_s)}{\partial n_s^2} = \frac{1}{D_0} - 2c^2 (n_s - n_s^*) \frac{c}{j\sqrt{\pi}} e^{-c^2(n_s - n_s^*)^2} + \frac{f(N_c)\Delta t}{p_{\text{st}}(n_s)} \left\{ -2c^2 + \left[\frac{j}{D_0 p_{\text{st}}(n_s)} - 2c^2 (n_s - n_s^*) \right] \times \left[\frac{2j}{D_0 p_{\text{st}}(n_s)} - 2c^2 (n_s - n_s^*) \right] \right\}. \quad (\text{A.7})$$

Next, we assume that the stationary probability distribution close to the top of the barrier can be approximated by the equilibrium distribution:

$$p_{\text{st}}(n_s) \approx p_{\text{eq}}(n_s) = Z^{-1} e^{-\beta U(n_s)} \approx Z^{-1} e^{-\beta U(n_s^*) + c^2(n_s - n_s^*)^2}, \quad (\text{A.8})$$

where $Z = \int_a^b dz e^{-\beta U(z)}$ is the normalization factor of a probability distribution defined on an interval (a, b) . In addition, we assume that the reaction rate is well approximated by classical nucleation theory,

$$j \approx \frac{c}{\sqrt{\pi}} e^{-\beta U(n_s^*)}, \quad (\text{A.9})$$

and ignore all terms $\sim D_0^{-1}$. In this way, we obtain a quadratic equation for the position of the inflection point,

$$\tilde{n}_s(N_c) = n_s^* + \frac{\sqrt{\pi} Z^{-1}}{2c^2 \Delta t f(N_c)} \left\{ 1 \pm \sqrt{1 + \frac{8 [c \Delta t f(N_c)]^2}{\pi Z^{-2}}} \right\}. \quad (\text{A.10})$$

-
- ¹ C. Dellago and P. G. Bolhuis, *Advanced Computer Simulation Approaches for Soft Matter Sciences III, Advances in Polymer Science* (Springer, New York) **221**, 167 (2009).
- ² T. S. van Erp and P. G. Bolhuis, *J. Comput. Phys.* **205**, 157 (2005).
- ³ R. J. Allen, C. Valeriani, and P. R. ten Wolde, *J. Phys.: Condens. Matter* **21**, 463102 (2009).
- ⁴ S. Bonella, S. Meloni, and G. Ciccotti, *Eur. Phys. J. B* **85**, 97 (2012).
- ⁵ R. Landauer, in *Noise in nonlinear dynamical systems*, Vol. 1. Theory of continuous Fokker-Planck systems, edited by F. Moss and P. V. E. McClintock (Cambridge University Press, 1989).
- ⁶ H. A. Kramers, *Physica* **7**, 284 (1940).
- ⁷ J. S. Langer, *Ann. Phys.* **54**, 258 (1969).
- ⁸ P. Talkner, *Z. Phys. B – Condens. Matter* **68**, 201 (1987).
- ⁹ P. Hänggi, P. Talkner, and M. Borkovec, *Rev. Mod. Phys.* **62**, 251 (1990).
- ¹⁰ D. J. Bicout and A. Szabo, *J. Chem. Phys.* **106**, 10292 (1997).
- ¹¹ J. M. Rubí and A. Pérez-Madrid, *Physica A* **298**, 177 (2001).
- ¹² S. Park, M. K. Sener, D. Lu, and K. Schulten, *J. Chem. Phys.* **119**, 1313 (2003).
- ¹³ A. Berezhkovskii and A. Szabo, *J. Chem. Phys.* **122**, 014503 (2005).
- ¹⁴ D. Reguera, J. M. Rubí, and J. M. G. Vilar, *J. Phys. Chem. B* **109**, 21502 (2005).
- ¹⁵ L. S. Bartell and D. T. Wu, *J. Chem. Phys.* **125**, 194503 (2006).
- ¹⁶ J. Wedekind, R. Strey, and D. Reguera, *J. Chem. Phys.* **126**, 134103 (2007).
- ¹⁷ J. Wedekind and D. Reguera, *J. Phys. Chem. B* **112**, 11060 (2008).
- ¹⁸ G. Chkonia, J. Wölk, R. Strey, J. Wedekind, and D. Reguera, *J. Chem. Phys.* **130**, 064505 (2009).
- ¹⁹ S. E. M. Lundrigan and I. Saika-Voivod, *J. Chem. Phys.* **131**, 104503 (2009).
- ²⁰ V. G. Baidakov, A. O. Tipseev, K. S. Bobrov, and G. V. Ionov, *J. Chem. Phys.* **132**, 234505 (2010).
- ²¹ V. G. Baidakov and A. O. Tipseev, *Thermochimica Acta* **522**, 14 (2011).
- ²² V. G. Baidakov, K. S. Bobrov, and A. S. Teterin, *J. Chem. Phys.* **135**, 054512 (2011).
- ²³ V. G. Baidakov and A. O. Tipseev, *J. Chem. Phys.* **136**, 074510 (2012).
- ²⁴ A. V. Mokshin and B. N. Galimzyanov, *J. Phys. Chem. B* **116**, 11959 (2012).
- ²⁵ A. V. Mokshin and B. N. Galimzyanov, *J. Chem. Phys.* **140**, 024104 (2014).
- ²⁶ V. A. Shneidman, *J. Chem. Phys.* **141**, 051101 (2014).
- ²⁷ P. R. ten Wolde, M. J. Ruiz-Montero, and D. Frenkel, *J. Chem. Phys.* **104**, 9932 (1996).
- ²⁸ D. Moroni, P. R. ten Wolde, and P. G. Bolhuis, *Phys. Rev. Lett.* **94**, 235703 (2005).
- ²⁹ G. T. Beckham and B. Peters, *J. Phys. Chem. Lett.* **2**, 1133 (2011).
- ³⁰ S. Jungblut, A. Singraber, and C. Dellago, *Mol. Phys.* **111**, 3527 (2013).
- ³¹ P. J. Steinhardt, D. R. Nelson, and M. Ronchetti, *Phys. Rev. B* **28**, 784 (1983).
- ³² H. C. Andersen, *J. Chem. Phys.* **72**, 2384 (1980).
- ³³ T. S. van Erp, D. Moroni, and P. G. Bolhuis, *J. Chem. Phys.* **118**, 7762 (2003).
- ³⁴ D. Moroni, T. S. van Erp, and P. G. Bolhuis, *Phys. Rev. E* **71**, 056709 (2005).
- ³⁵ S. Jungblut and C. Dellago, *J. Chem. Phys.* **134**, 104501 (2011).
- ³⁶ L. S. Pontryagin, A. A. Andronov, and A. A. Vitt, *JETP* **3**, 165 (1933), reproduced in *Noise in nonlinear dynamical systems*, Vol. 1. Theory of continuous Fokker-Planck systems, edited by F. Moss and P. V. E. McClintock (Cambridge University Press, 1989).
- ³⁷ D. Boilley, B. Jurado, and C. Schmitt, *Phys. Rev. E* **70**, 056129 (2004).
- ³⁸ S. Jungblut and C. Dellago, *EPL* **96**, 56006 (2011).
- ³⁹ W. Ostwald, *Z. Phys. Chem.* **22**, 289 (1897).
- ⁴⁰ I. N. Stranski and D. Totomanow, *Z. Phys. Chem.* **163**, 399 (1933).
- ⁴¹ M. von Smoluchowski, *Wien. Sitz. Ber.* **124**, 339 (1915).
- ⁴² H. Risken, *The Fokker-Planck Equation* (Springer-Verlag Berlin Heidelberg, 1989, 1996).
- ⁴³ B. Peters, P. G. Bolhuis, R. G. Mullen, and J. Shea, *J. Chem. Phys.* **138**, 054106 (2013).
- ⁴⁴ D. E. Makarov, *J. Chem. Phys.* **138**, 014102 (2013).
- ⁴⁵ V. Balakrishnan, G. Nicolis, and C. Nicolis, *Phys. Rev. E* **61**, 2490 (2000).
- ⁴⁶ M. Kac, *Bull. Amer. Math. Soc.* **53**, 1002 (1947).